Analytical Methods

Accepted Manuscript

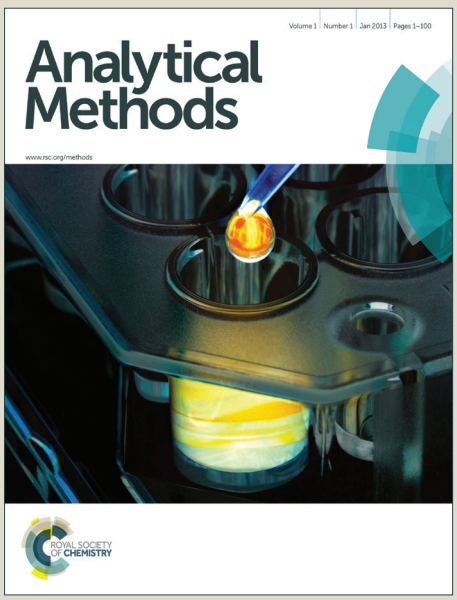

ROYAL SOCIETY OF CHEMISTRY

www.rsc.org/methods

Cite this: DOI: 10.1039/c0xx00000x

www.rsc.org/xxxxxx

ARTICLE TYPE

Mass spectrometry-based lipidomics analysis using methyl tert-butyl ether extraction in human hepatocellular carcinoma tissues

Shuxia Jiang[a,b], Yongle Li[c], Shuhai Lin[b], Hongbo Yang[c], Xin-yuan Guan[d], Haiyun Zhou[a,*], Tiangang Luan[a,e], Zongwei Cai[b,*]

Received (in XXX, XXX) Xth XXXXXXXXX 20XX, Accepted Xth XXXXXXXXX 20XX

DOI: 10.1039/b000000x

Hepatocellular carcinoma (HCC) is one of the most common cancers in human beings and not well treated. Due to its blurred biomarkers, lipidomics can be considered as a new diagnostic tool. In this study, mass spectrometry-based lipidomics analysis coupled with multivariate statistical analysis was applied to profile twelve pairs of human hepatocellular carcinoma tissues (HCT) and matched adjacent non-tumour tissues (ANT). As a result, perturbation of lipid biosynthesis was observed in HCT compared to ANT. Lipid species were profiled and 28 significant lipids were identified based on high resolution mass spectrometry with mass error less than 3 ppm, covering phosphatidylcholine (PC), phosphatidylethanolamine (PE), phosphatidylglycerol (PG), phosphatidylinositol (PI), sphingomyelin (SM) and triglyceride (TG). High mass accuracy as well as tandem MS (MS/MS) technique provides high confidence of lipid identification. Interestingly, the decreased PGs and PIs were observed in this study, indicating that lipolysis of PGs and PIs might play a crucial role in HCC development. Results indicated that mass spectrometry-based lipidomics analysis could serve as an effective means to diagnose canceration.

1 Introduction

Hepatocellular carcinoma (HCC) is one of the most common causes of death from cancer in human beings, and the incidence increase per year. It was the fifth malignancy in men and the eighth in women around the world in 2000,[1] but it was the second cause of cancer death in 2012.[2] The main reason for the increase is either infection with hepatitis B and C viruses (HBV and HCV) or cirrhosis. It's hard to cure HCC, so the early detection and diagnosis is becoming increasingly important. Metabolites in pathological organism are irregular which could be used as potential biomarkers to predict pathological changes. To understand the disturbed metabolites in pathological liver, metabolomics and lipidomics are considered to be valuable tools.

Lipidomics was put forward as a branch of metabolomics and was defined as "the full characterization of lipid molecular species and of their biological roles with respect to expression of proteins involved in lipid metabolism and function, including gene regulation".[3] It focused on full analysis of lipid species and their biological significance in regard to health and diseases through a knowledge of proteins, genes and other relative factors.

Lipids are mainly divided into eight categories including fatty acyls (FA), glycerolipids (GL), glycerophospholipids (GP), sphingolipids (SP), sterol lipids (ST), prenol lipids (PR), saccharolipids (SL), and polyketides (PK). This classification not only covers eukaryotic but also prokaryotic source.[4] Alteration of lipid metabolism in cancer cells has been observed under hypoxia or metabolic stress. To address the lipid species, lipidomics enables identification and quantification of lipid species for understanding pathogenesis in human diseases.[5-8]

Because of the diversity and complexity of lipids, many analytical methods have been developed, including thin-layer chromatography (TLC),[9] gas chromatography mass spectrometry (GC-MS),[10] liquid chromatography mass spectrometry (LC-MS),[11] and nuclear magnetic resonance (NMR).[12] Compared to other methods, chromatography-mass spectrometry has general applicability with high resolution, high throughput, high sensitivity and specificity, which make it become one of the major analytical tools. Numerous LC-MS methods were applied in analysing cellular and tissular lipids.[7, 13, 14] Along with the development of analysis methods, extraction methods were also improved. Vitali Matyash et al. have put forward a new method using methyl tert-butyl ether (MTBE) as extraction solvent.[15] MTBE is relatively non-toxic and non-carcinogenic.[16] Due to its low density, MTBE locates in the upper phase when mixing with methanol and water. The non-extractable debris were kept at the bottom away from extractable lipids. This advantage make it easy to transfer upper MTBE phase with extractable lipids. In term of chloroform, it has higher density than those of methanol and water. When using chloroform/methanol as extraction solvent, the organic phase will locate at the bottom, and the non-extractable debris will be kept in the middle layer between

[a] *Instrumental Analysis & Research Center, Sun Yat-sen University, Guangzhou, 510275, China. E-mail: zhouhy@mail.sysu.edu.cn.*

[b] *State Key Laboratory of Environmental and Biological Analysis and Department of Chemistry, Hong Kong Baptist University, Kowloon, Hong Kong SAR, China. Fax: +852-3411 7348; Tel: +852-3411 7070; E-mail: zwcai@hkbu.edu.hk*

[c] *Shenzhen Academy of Metrology and Quality Inspection, Shenzhen, 518000, China*

[d] *Department of Clinical Oncology, Li Ka Shing Faculty of Medicine, the University of Hong Kong, Hong Kong SAR, China*

e MOE Key Laboratory of Aquatic Product Safety, School of Life Sciences, Sun Yat-sen University, Guangzhou, 510275, China

organic phase and the upper water phase. While collecting lipid species from the bottom organic phase, the pipette will easily be contaminated by the upper water phase and the non-extractable debris. Furthermore, the carcinogenicity of chloroform is a big health hazardous problem to the operators.

Although lipidomics has been studied for decades, the biological significance of lipids in HCC has not been characterized clearly. In present study, MTBE was used to extract lipids, and ultrahigh performance liquid chromatography coupled with high resolution mass spectrometry Orbitrap XL was employed to analyse lipids of hepatocellular carcinoma tissues (HCT) compared to matched adjacent tissues (ANT). Multivariate statistical analysis was performed for grouping and feature selection, and MS/MS with online database were utilized to identify remarkable lipid species.

2 Experimental

2.1 Reagents and chemicals

Methyl alcohol, chloroform, acetonitrile and isopropyl alcohol, as well as formic acid were purchased from TEDIA (Fairfield, OH, USA). Tert-butyl methyl ether (MTBE) and ammonium acetate were obtained from Sigma–Aldrich (St. Louis, MO, USA), ultrapure water was prepared from a Milli-Q system (Millipore, USA). Other reagents were analytical grade.

2.2 Sample preparation

A total of 12 HCC patients, who underwent hepatectomy at Sun Yat-sen University Cancer Center (Guangzhou, China), were included in this study. Tissue samples used in this study were approved by the Committees for Ethical Review of Research involving Human Subjects at Cancer Center of Sun Yat-sen University. MTBE was used to extract lipids from the samples, and the proportion of MTBE, methanol and water is designed based on Vitali Matyash's method.[15] The optimized extraction steps are as follows: about 50 mg of each tissue were weighed and quick-frozen by liquid nitrogen. 100 μL of ice-chilled water and 300 μL of cold methanol were added for stir homogenizer. Then 1 mL of MTBE was added to the mixture and incubated at −20 °C for 1 h. Followed by addition of 150 μL H_2O, samples were incubated at −20 °C for another 15 min, hereafter centrifuged at 12000 rpm for 10 min at 4 °C. The organic phase was transferred to a new Eppendorf tube and stored at −20 °C. The lower phase was re-extracted with 400 μL of a MTBE/methanol/water mixture (10:3:2.5, v/v/v). The organic phase from twice extractions was combined and dried under gentle nitrogen stream. The residue was stored at −80 °C for further analysis.

2.3 LC-MS analysis

UPLC-Orbitrap XL mass spectrometer (Thermo Fisher Scientific) was used for lipid analysis with minor modification according to a previously published method.[17] Samples were reconstituted in 50 μL of chloroform/methanol (2:1, v/v) and diluted five times in acetonitrile/isopropanol/water (65:30:5, v/v/v). After centrifuged for 15 min at 4 °C, the supernatant was moved to sample vials. Chromatographic separation was performed on a reversed phase UPLC ACQUITY C18 column (2.1 mm × 50 mm × 1.7 μm, Waters, USA).

Mass spectrometric detection was first performed with electrospray ionization (ESI) in positive mode. Mobile phase A was 60% acetonitrile in water, containing 10 mM ammonium acetate and 0.05% formic acid, and B was isopropanol/acetonitrile (9:1, v/v). The flow rate was 200 μL/min, with the elution gradient as follows: 25% B was firstly maintained for 1 min, linearly increased to 50% B in 2 min, then to 97% B in 16 min and maintained for 4 min followed by equilibration with 25% B and maintained for 6 min. Survey full-scan MS spectra (mass range *m/z* 400 to 1200) were acquired with resolution R=30,000 at *m/z* 400. The source voltage, capillary temperature, sheath gas flow, auxiliary gas flow and tube lens were set at 3 kV, 300 °C, 35 arb, 5 arb and 60 V, respectively. The MS/MS identification was performed using normalization collision induced dissociation (CID), the collisional energy was between 20 % and 35 %.

The analysis was also performed in negative mode. The gradient program and mobile phase are the same as those at positive mode. Source voltage, capillary temperature, sheath gas flow, auxiliary gas flow and tube lens were set at 2.5 kV, 300 °C, 50 arb, 5 arb and -100 V, respectively. MS/MS was also implemented.

The stabilities of retention time, signal intensity and mass accuracy are essential during a continuous LC-MS analysis with a repeated method. A quality control (QC) sample was therefore prepared in order to investigate the stability of the instrument and ensure the reliability of the data. The QC sample was prepared by mixing equivalent volume (10 μL) of all samples in the study. QC injections were set in every eight sample runs in the sample run sequence. QC sample was also ran before and after the sequence in order to assess repeatability of the data.

External mass calibration was applied to ensure mass accuracy of the mass spectrometer before every sequence ran.

2.4 Data processing and analysis

The raw data were acquired and aligned using the R statistical programming environment (http://www.r-project.org) based on unique *m/z* value and retention time (RT). The "80% rule"[18] was applied to exclude missing values, i.e., variables were removed if their nonzero values were presented in less than 80% in both studied groups simultaneously. The statistical significance was calculated using the student's t-test, and features were chose under the condition of *P*-value < 0.05 and fold-change > 1.5. Intensities of ions from both positive mode and negative mode with statistical significance were merged and imported into the SIMCA-P program (version 11.0, Umetrics) for multivariate analysis. Principal component analysis (PCA) and partial least squares discriminate analysis (PLS-DA) were calculated with pareto scaling. The preliminary identification of parent ions was searched against online databases such as METLIN (http://metlin.scripps.edu/), and further identification was based on MS/MS fragments. GraphPad Prism (version 5, GraphPad Software, Inc., La Jolla, CA) was used to compare the results for paired HCT and ANT.

3 Results and Discussion

3.1 Optimization of LC-MS chromatogram

Samples were analysed by UPLC-MS in the mode of profiling, and numerous lipid species were detected, including phosphatidylcholine (PC), phosphatidylethanolamine (PE), phosphatidylinositol (PI), phosphatidylglycerol (PG), phosphatidylserine (PS), sphingomyelin (SM), triacylglycerol (TG). Full scan base peak mass chromatogram of lipid metabolites of QC sample in positive mode is presented in Fig. 1. And the typical full scan base peak mass chromatogram of samples of the ANT group and HCT group are shown in supplementary information (Fig. S1). Lipids were eluted mainly between 8 and 20 min. The longer alkyl chain, the higher the degree of unsaturation, the longer retention time. Therefore PCs, PEs, PIs, PGs, PSs and SMs were mainly detected within 8-16min, while TGs were detected at 16-20 min. Due to nonpolar extraction, lysoPCs and lysoPEs were not detected under current chromatographic condition. In addition, glycerophospholipids have two alkyl chain with different phospholipid head, their similar structure led to closer retention time and formed co-current peaks.

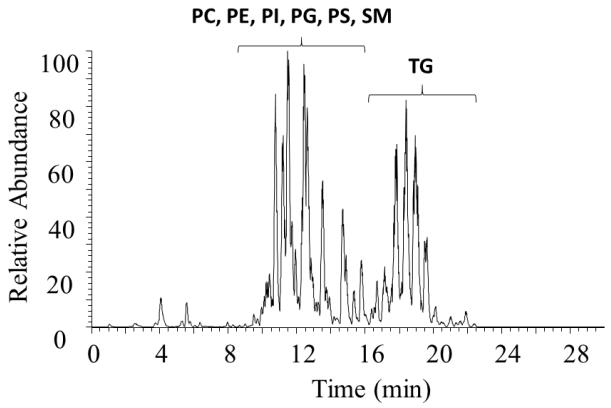

Fig. 1. Full scan base peak mass chromatogram of the QC sample in positive mode. (PC, phosphatidylcholine; PE, phosphatidylethanolamine; PI, phosphatidylinositol; PG, phosphatidylglycerol; PS, phosphatidylserine; SM, sphingomyelin; TG, triacylglycerol).

3.2 Multivariate analysis

Two contrastive groups were analysed both in positive and negative full scan mode. Excel data containing retention time and ion intensity were obtained by using R statistical programming environment (http://www.r-project.org), and then imported into SIMCA-P program (version 11.0, Umetrics) for PCA (Fig. 2A, 2B). The score plots in the figure contain HCT group, ANT group and QC group. It can be seen that all samples were scattered in the figure, being clearly classified with all subjects fell into the 95% confidence interval basically. ANT group and HCT group were clustered together respectively and separated from each other. QC group mainly gathered together, indicating the instrument had good stability and repeatability.

For further analysis, PLS-DA, a supervised statistical method, was applied to the classification of HCT group and ANT group. Scores plots in both positive and negative mode showed a better clustering and separation between HCT group and ANT group in the PLS-AD. The fraction of the sum of squares R2Y were 0.994 and predicted residual sum of squares Q2 (cum) were 0.923 in positive mode (Fig. 2C). Values of R2Y and Q2 (cum) close to 1.0 indicated an excellent model. Model validation was also carried out by permutation testing, which is one of the established methods of internal validation. 999 random model permutations were used for permutation analysis. The goodness of fit (R2) and predictive ability (Q2) of the original models indicated on the top right corner were higher than those of 999 permuted models to the left (Fig. 2D). This demonstrated the valid of the model used for the comparison of HCT group and ANT group. Multivariate analysis exhibited marked metabolic differences between the two groups.

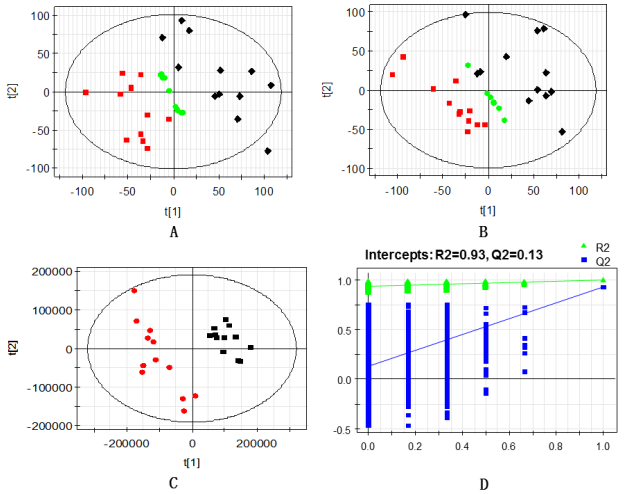

Fig. 2. The red scores represent ANT group, the black scores represent HCT group, and the green scores represent QC group. A: PCA of positive mode; B: PCA of negative mode; C: PLS-DA of positive mode; D: Permutations analysis by using 999 random model permutations in positive mode.

3.3 Potential biomarker identification

The format of raw data were converted into mzXML by using MassMatrix Mass Spec Data File Conversion Tools, then merged and imported into R software package to obtain the information of all peaks. After screened by using "80% rule", the rest of the ions which met the conditions of *P*-value < 0.05, and fold-change > 1.5, were imported into online database to search and match. Numerous ions were maintained as significant quasi-molecular ions with mass error less than 5 ppm. Parent ions together with their MS/MS fragment ions were used for the compound identification with the help of online databases.

For instance, peak at RT 16.63 min with $[M+H]^+$ ion *m/z* 823.68 was identified as TG (16:1/16:1/18:4). The ion *m/z* 823.68056 was imported into METLIN metabolite database and a series of isomeric TGs were obtained. Mass deviation and fatty acid chains were used for further inference. The parent ion *m/z* 823.68 produced fragment ions at *m/z* 569.45 and *m/z* 547.47 after neutral losses of *m/z* 254.23 and *m/z* 276.21, respectively, in its MS/MS spectrum. By calculating the mass and unsaturation degree of the neutral loss, fatty acid chain (16:1) and fatty acid chain (18:4) were obtained. The fatty acid chains and ion

fragments obtained in the experiment were completely consistent with the fragment loss values from TG (16:1/16:1/18:4). Therefore, the peak at 16.63 min with *m/z* 823.68 was characterized as TG (16:1/16:1/18:4) (Fig. 3).

Using the same method mentioned above, 28 metabolites were identified with mass error less than 3 ppm. In general, TGs were detected in positive mode in the form of $[M+H]^+$ while PGs and PIs were better ionized in negative mode giving the ions of $[M-H]^-$ (Table 1, 2).

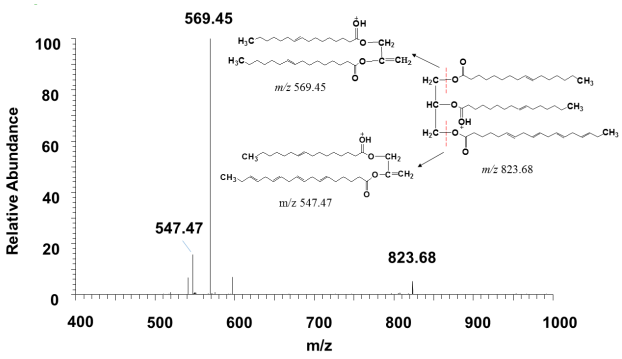

Fig. 3. MS/MS spectrum of the metabolite at *m/z* 823.68.

Table 1. Significant metabolites identified in positive mode

Metabolites	$[M+H]^+$	RT(min)	Fragment Ions	*P*-value	Fold	Mass error (ppm)	Change trend
DG(12:0/22:3)	591.49686	13.65	335.26	2.10×10^{-6}	5.33	2	↑
SM(d20:0/24:1)	843.72979	16.16	825.70/545.46	4.10×10^{-5}	2.82	1	↓
TG(16:0/16:0/18:1)	833.76213	18.62	577.52/551.50	4.32×10^{-3}	1.35	0	↑
TG(16:0/18:0/18:3)	857.75944	19.25	601.52/573.49	8.28×10^{-3}	1.83	0	↑
TG(16:0/18:1/20:4)	881.75830	18.85	625.52/599.50/577.52	5.97×10^{-8}	2.18	1	↓
TG(16:0/18:2/20:5)	877.72699	17.42	621.48/597.48/575.50	5.03×10^{-8}	1.81	2	↓
TG(16:0/18:3/20:5)	875.71147	16.67	619.47/597.48	1.74×10^{-8}	2.21	0	↓
TG(16:1/16:1/18:4)	823.68056	16.63	569.45/547.47	6.74×10^{-3}	1.63	0	↑
TG(16:1/18:2/20:5)	875.71184	16.94	621.48/595.47/573.49	2.23×10^{-6}	2.29	2	↓
TG(20:4/18:2/20:5)	925.72721	16.48	645.48/621.48	3.93×10^{-9}	2.15	2	↓

Abbreviations: RT, retention time; fold, fold change; ↑, upregulated; ↓, downregulated.

Table 2. Significant metabolites identified in negative mode

Metabolites	$[M-H]^-$	RT (min)	Fragment Ions	*P*-value	Fold	Mass error (ppm)	Change trend
PC(22:6/15:0)	790.54096	12.47	327.23/480.31	3.99×10^{-4}	1.97	2	↓
PE(20:3/16:0)	740.52547	12.34	305.25/255.23/452.28	4.07×10^{-2}	1.73	2	↑
PE(20:4/18:0)	766.54131	12.78	303.24/480.31	1.54×10^{-2}	2.10	2	↑
PE(22:5/16:0)	764.52513	12.74	329.25	3.82×10^{-2}	1.51	2	↑
PE(22:6/16:0)	762.50948	11.39	255.23/327.23	2.31×10^{-4}	2.17	2	↓
PG(18:1/18:1)	773.53521	10.81	281.25	2.02×10^{-3}	1.88	1	↓
PG(18:1/18:2)	771.51931	9.78	279.23/281.25	2.80×10^{-4}	2.24	1	↓
PG(18:1/20:4)	795.51926	9.56	303.23/281.25	3.19×10^{-2}	1.61	1	↓
PG(18:2/18:2)	769.50350	8.89	279.23	5.68×10^{-5}	3.42	1	↓
PG(18:2/18:3)	767.48822	8.08	277.22/279.23	2.18×10^{-4}	5.08	1	↓
PG(18:2/20:4)	793.50339	8.65	303.23/279.23	5.03×10^{-5}	2.57	1	↓
PG(18:2/22:5)	819.51916	9.21	279.23/329.25	9.66×10^{-4}	1.83	1	↓
PG(18:2/22:6)	817.50331	8.33	279.23/327.23	2.37×10^{-4}	2.59	0	↓
PI(16:0/18:2)	833.51963	10.49	553.28/391.23	1.34×10^{-3}	2.49	1	↓
PI(18:0/18:2)	861.55053	11.63	581.31	7.22×10^{-3}	3.29	0	↓
PI(18:0/20:4)	885.55013	11.33	581.31	1.87×10^{-2}	1.60	0	↓
PI(20:4)/16:0)	857.51934	10.24	553.28/391.23	4.10×10^{-2}	1.29	1	↓
PI(20:4/17:0)	871.53503	10.86	567.30/303.23/269.25	8.13×10^{-3}	1.60	0	↓

Abbreviations: RT, retention time; fold, fold change; ↑, upregulated; ↓, downregulated.

All the identified metabolites stated both down and upregulation, as shown in table 1 and 2. The majority of the important metabolites were decreased in HCT compared to ANT. Five TGs have shown downregulated and three TGs shown upregulated. As to DG (12:0/22:3), SM (d20:0/24:1) and PC (22:6/15:0), the

increasing of DG (12:0/22:3) and the decreasing of SM (d20:0/24:1) and PC (22:6/15:0) were observed. Although most of the lipids were downregulated, PEs were mainly ascend except PE (22:6/16:0). What is needed to be addressed is that in all the metabolites identified, PGs and PIs both showed a consistent downward trend as depicted in Fig. 4. In addition, the *P*-values of PGs and PIs were mainly less than 0.01, suggesting that PGs and PIs had significance in the metabolic profile.

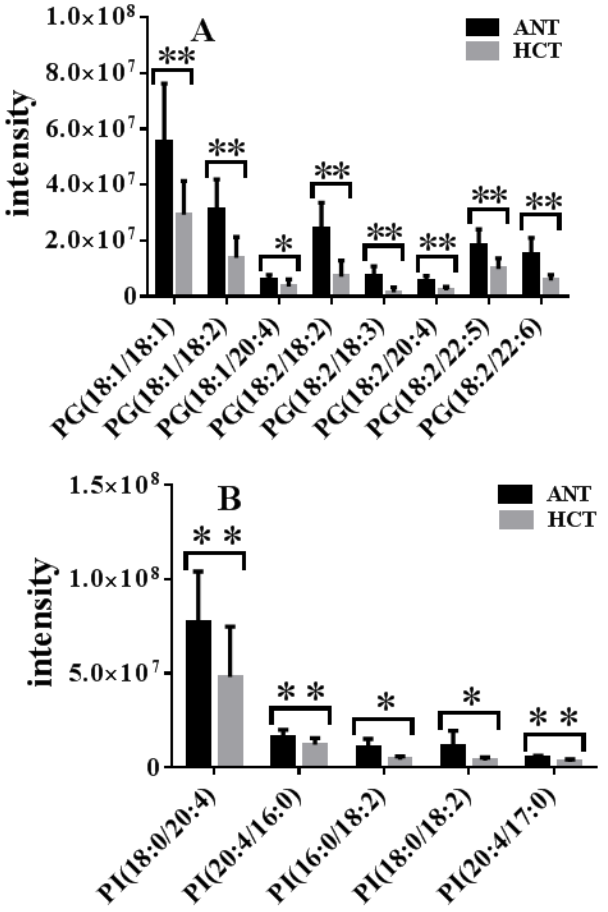

Fig. 4. PG and PI showed the downregulation in HCT (12 cases) tissues compared to ANT (12 cases). The data are expressed as mean value ± SD (* means *P*-value< 0.05, ** means *P*-value < 0.01).

3.4 Analysis of the biological significance of lipids

Glycerolipids (*mono-, di-* or *tri-*) are mainly biosynthesized through sn-glycerol-3-phosphate pathway, which is the predomination in liver.[19] The synthesis pathway of TG is presented in the supplementary information (Fig. S2).[20] As the main source of energy in eukaryotic cells, TGs received much concern. Aberrant TGs metabolism were found in patients with cancer, for instance, studies showed that plasma TGs decreased in HCC patients.[21] In this study, five TGs including TG (16:0/18:1/20:4), TG (16:0/18:2/20:5), TG (16:0/18:3/20:5), TG (16:1/18:2/20:5) and TG (20:4/18:2/20:5) were decreased in HCT compared with ANT. Three TGs including TG (16:0/16:0/18:1), TG (16:0/18:0/18:3), TG (16:1/16:1/18:4) and one DG (12:0/22:3) were increased. It can be illuminated that sn-glycerol-3-phosphate pathway has been disturbed in HCC patients.

Sphingolipid synthesis pathway is also disturbed, because SM (d20:0/24:1) was found decreased in HCC patients. Studies showed that the levels of SM in human cancer cells were lower than non-tumour cells and the deactivation of SM synthases on account of the decrease of SM levels.[22] Chen et al[14] also reported that plasma SMs were remarkable downregulated in HCC patients.

Pathway of glycerophospholipds is intricate. PCs are generated from Kennedy pathway, as well as PEs. And PEs are also synthesized from PSs through CDP-DAG pathway[6] (supplementary information, Fig. S3). It had been demonstrated that PEs were significantly greater in HCT,[7] exactly as showed in this research that PEs were mainly increased in HCT. Three PEs including PE (20:3/16:0), PE (20:4/18:0) and PE (22:5/16:0) were increased and one PE (22:6/16:0) was decreased. Only one PC (22:6/15:0) was identified in this study, and it showed downregulated. Polyunsaturated PCs were mainly synthesized from PEs catalysed by phosphatidylethanolamine (PEMT). This result was consistent with the research that the activity of PEMT was lower in HCC patients compared with healthy controls.[23]

PIs and PGs are synthesized through CDP-DAG pathway in the endoplasmic reticulum.[24, 25] The enzyme CDP-diacylglycerol synthetase (CdsA) plays a crucial role in regulating PIs and PGs, its decreased activity will cause the reduction of PIs and PGs.[26] Deregulation of phosphoinositide metabolism is responsible for a number of human diseases, including cancer.[27] In the urine of patients with prostate cancer, PIs and PGs decreased obviously.[28] PGs and PIs were also found highly descend in HCT in present study results (Fig. 4). These results indicate that CdsA in the CDP-DAG pathway might be disturbed in HCC patients.

4. Conclusions

Tissue metabolites can supply direct information metabolic deregulation. This article shows MTBE solvent for tissues extraction and profiling with high accuracy mass spectrometry and mainly long-chain lipids were detected. HCT and ANT were studied with 28 significant lipids identified including DGs, SMs, TGs, PCs, PEs, PGs and PIs. Profiling of lipids revealed a great change between HCT and ANT, indicating that mass spectrometry-based lipidomics analysis provides a new insight for the phenotypes of liver cancer.

Acknowledgements

The authors would like to thank financial support from Collaborative Research Fund (HKBU5/CRF/10) of Hong Kong Research Grant Council and National Natural Science Foundation of China (NSFC-21377106).

References

1. F. X. Bosch, J. Ribes, M. Diaz and R. Cleries, *Gastroenterology*, 2004, **127**, S5-S16.
2. .I. A. f. R. o. Cancer, *Effective prevention measures urgently needed to prevent cancer crisis (Press Release No. 224)*, 2014.
3. F. Spener, M. Lagarde, A. Géloên and M. Record, *Eur. J. Lipid Sci. Tech.*, 2003, **105**, 481-482.
4. E. Fahy, S. Subramaniam, R. C. Murphy, M. Nishijima, C. R. Raetz, T. Shimizu, F. Spener, G. van Meer, M. J. Wakelam and E. A. Dennis, *J. Lipid Res.*, 2009, **50 Suppl**, S9-14.
5. C. Hu, M. Hoene, X. Zhao, H. U. Haring, E. Schleicher, R. Lehmann, X. Han, G. Xu and C. Weigert, *PloS one*, 2010, **5**, e13318.
6. C. Huang and C. Freter, *Int. J. Mol. Sci.*, 2015, **16**, 924-949.

7. Q. Huang, Y. Tan, P. Yin, G. Ye, P. Gao, X. Lu, H. Wang and G. Xu, *Cancer Res.*, 2013, **73**, 4992-5002.
8. S. M. Lam and G. Shui, *J. Genet. Genomics.*, 2013, **40**, 375-390.
9. B. Fuchs, R. Suss, K. Teuber, M. Eibisch and J. Schiller, *J. Chromatogr. A*, 2011, **1218**, 2754-2774.
10. D. Beyoglu, S. Imbeaud, O. Maurhofer, P. Bioulac-Sage, J. Zucman-Rossi, J. F. Dufour and J. R. Idle, *Hepatology*, 2013, **58**, 229-238.
11. G. Shui, X. L. Guan, C. P. Low, G. H. Chua, J. S. Goh, H. Yang and M. R. Wenk, *Mol. Biosyst.*, 2010, **6**, 1008-1017.
12. Y. Yu, L. Vidalino, A. Anesi, P. Macchi and G. Guella, *Mol. Biosyst.*, 2014, **10**, 878-890.
13. Y. Shao, B. Zhu, R. Zheng, X. Zhao, P. Yin, X. Lu, B. Jiao, G. Xu and Z. Yao, *J. Proteome. Res.*, 2015, **14**, 906-916.
14. S. Chen, P. Yin, X. Zhao, W. Xing, C. Hu, L. Zhou and G. Xu, *Electrophoresis*, 2013, **34**, 2848-2856.
15. V. Matyash, G. Liebisch, T. V. Kurzchalia, A. Shevchenko and D. Schwudke, *J. Lipid Res.*, 2008, **49**, 1137-1146.
16. G. Gupta and Y. J. Lin, *B Environ Contam Tox*, 1995, **55**, 618-620.
17. S. Chen, M. Hoene, J. Li, Y. Li, X. Zhao, H. U. Haring, E. D. Schleicher, C. Weigert, G. Xu and R. Lehmann, *J. Chromatogr. A*, 2013, **1298**, 9-16.
18. A. K. Smilde, M. J. van der Werf, S. Bijlsma, B. J. van der Werff-van der Vat and R. H. Jellema, *Anal. Chem.*, 2005, **77**, 6729-6736.
19. K. Athenstaedt and G. Daum, CMLS-*Cell Mol. Life S.*, 2006, **63**, 1355-1369.
20. R. A. Coleman and D. G. Mashek, *Chem Rev*, 2011, **111**, 6359-6386.
21. M. Motta, I. Giugno, P. Ruello, G. Pistone, I. Di Fazio and M. Malaguarnera, *Minerva. Med.*, 2001, **92**, 301-305.
22. G. Barcelo-Coblijn, M. L. Martin, R. F. de Almeida, M. A. Noguera-Salva, A. Marcilla-Etxenike, F. Guardiola-Serrano, A. Luth, B. Kleuser, J. E. Halver and P. V. Escriba, *P. Natl. Acad. Sci. U.S.A.*, 2011, **108**, 19569-19574.
23. L. Tessitore, B. Marengo, D. E. Vance, M. Papotti, A. Mussa, M. G. Daidone and A. Costa, *Oncology-Basel*, 2003, **65**, 152-158.
24. Y. Y. Chang and E. P. Kennedy, *J. Lipid Res.*, 1967, **8**, 447-455.
25. B. W. Agranoff, R. M. Bradley and R. O. Brady, *J. Biol. Chem.*, 1958, **233**, 1077-1083.
26. Y. Liu, W. Wang, G. Shui and X. Huang, *PLoS Genet.*, 2014, **10**, e1004172.
27. T. Balla, *Physiol. Rev.*, 2013, **93**, 1019-1137.
28. H. K. Min, S. Lim, B. C. Chung and M. H. Moon, *Anal. Bioanal. Chem.*, 2011, **399**, 823-830.

Lipidomics was applied to analyse irregular metabolites in HCC tissues through LC-MS method which revealed a great changes between HCT compared to ANT.